Pathway Study on Dielectric Barrier Discharge Plasma Conversion of Hexane

Anıl Ağıral,*,†,‡ Cassia Boyadjian,§ K. Seshan,§ Leon Lefferts,§ and J. G. E. (Han) Gardeniers†

Mesoscale Chemical Systems, MESA+ Institute for Nanotechnology, Faculty of Science and Technology, University of Twente, PO Box 217, 7500 AE, Enschede, The Netherlands, Physical Biosciences Division, Lawrence Berkeley National Laboratory, One Cyclotron Road, Berkeley, California, 94720, United States, and Catalytic Processes and Materials, MESA+ Institute for Nanotechnology, IMPACT, Faculty of Science and Technology, University of Twente, PO Box 217, 7500 AE, Enschede, The Netherlands

Received: May 21, 2010; Revised Manuscript Received: October 5, 2010

A plasma reactor based on dielectric barrier discharge has been developed for oxidative cracking of hexane to yield olefins at atmospheric pressure. Dissociation of hexane in the presence of oxygen with nonequilibrium plasma state represents complex chemistry, and both conversion and product selectivities differ significantly from the thermodynamic equilibrium state. In order to understand plasma chemistry initiated by electron impact processes, the Boltzmann equation is solved to determine the average electron energy and energy fractions in collision processes. Activation of oxygen in the plasma brings a new route with electron impact dissociation yielding atomic oxygen radicals and initiates oxidative cracking of hexane. Changes in certain features of the dissociation pattern of hexane to yield olefin products with varying parameters such as temperature, oxygen addition, and helium concentration are discussed.

1. Introduction

There is an enormous and ever-increasing demand for ethylene and propylene, which are important building blocks for the chemical industry, with a predicted growth rate of 4% for the coming years.[1] It is expected that the propylene demand will grow faster than that of ethylene. However, current process technology is unlikely to satisfy these high olefin demands.

Steam cracking is the major route for the production of olefins today. Light olefins are produced by cracking the hydrocarbon feedstock, e.g., ethane, LPG, or naphta, in the presence of steam at temperatures of 700−900 °C. Steam cracking is a highly endothermic reaction, requiring substantial energy input. Coke deposition on the walls of reactors inhibiting heat transfer is considered a significant issue.

One of the potential alternatives to steam cracking is catalytic oxidative cracking, which is exothermic, has minimal coke formation, while the energy required for cracking can be generated internally. Liu et al.[2] observed that during noncatalytic pyrolysis of hexane at 750 °C, in the presence of oxygen, a high conversion of hexane of 85 mol % with reasonable total olefin selectivity can be obtained, resulting in about 59 mol % selectivity to light olefins. The cracking process was allowed to run in an autothermal way with oxygen, where exothermic combustion of product hydrogen provided the heat for cracking.

As yet another alternative, atmospheric pressure nonthermal plasma technology can be effectively used for cracking and dehydrogenation of hydrocarbons and introducing efficient chemical activation routes to break thermodynamic limitations.[3−7] Recently, it has been shown that a single step, noncatalytic, and selective synthesis of synthetic fuels (methanol, formaldehyde, and formic acid) via room temperature methane partial oxidation is feasible using atmospheric pressure dielectric barrier discharge.[5] Barrier discharge can be generated by placing a dielectric between the electrodes to protect the electrode from direct arc formation, and excess gas heating is avoided due to formation of nanosecond current pulses. Microdischarges, which are generated in the gas gap, allow plasma chemical conversion. In the discharge process, the cold plasma can provide a high electron temperature and the impact of energetic electrons with the reactant molecules can create active species, e.g., radicals and ions, at ambient gas temperatures. Therefore electrons, ions, and neutral species have different temperatures and kinetic energies.

Pierce et al.[8] proposed a dissociation model for pulsed hexane plasma, explaining the bond scission and dissociation pattern of hexane for an application of creating carbon films at ambient temperatures. Kudryashov et al.[9] studied the conversion of hexane in a barrier discharge to form branched-chain hydrocarbons and found that the efficiency of the barrier discharge can be increased by furnishing oxidative dimerization of hexane at room temperature. Similarly, microwave discharge induced dissociation of hexane that resulted from electron−molecule collisions and thermal reactions in the discharge zone, produced large branched hydrocarbons as well.[10] Conversion of hexane was also carried out in an alternating current discharge plasma with integrated catalytic electrodes in order to produce hydrogen and light alkanes and olefins, at room temperature and atmospheric pressure, for potential application in automotive exhaust gas purification.[11]

In this study, the application of a dielectric barrier discharge reactor for oxidative cracking of hexane is investigated in order to understand the conversion process to olefins. Our objective behind the application of discharge is to induce hexane dissociation at lower temperatures as compared to thermal activation. The effects of temperature, oxygen addition, and helium concentration on the dissociation patterns of hexane toward olefins will be interpreted on the basis of a plasma

* To whom correspondence should be addressed, aagiral@lbl.gov.
† Mesoscale Chemical Systems, MESA+ Institute for Nanotechnology, Faculty of Science and Technology, University of Twente.
‡ Physical Biosciences Division, Lawrence Berkeley National Laboratory.
§ Catalytic Processes and Materials, MESA+ Institute for Nanotechnology, IMPACT, Faculty of Science and Technology, University of Twente.

10.1021/jp104697u
Published on Web 10/20/2010

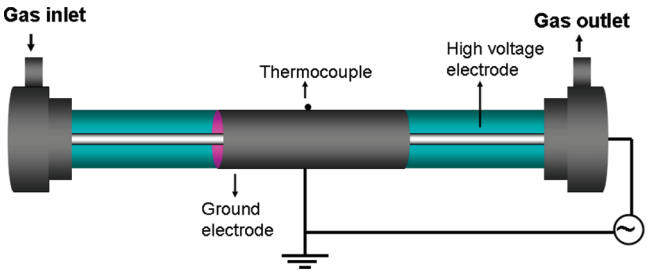

Figure 1. A schematic representation of the dielectric barrier discharge type plasma reactor.

chemistry model that describes the electron energy and species distribution over the different electron impact processes.

2. Experimental Section

Figure 1 shows a schematic representation of the dielectric barrier discharge (DBD) type plasma reactor. A discharge was generated between a high voltage wire electrode, to which a 6 kV peak ac voltage with 50 kHz frequency was applied, and a grounded aluminum metal foil which was positioned around a quartz tube. The diameters of the quartz tube reactor and high voltage wire electrode are 6.5 and 1.5 mm, respectively. The length of the grounded electrode is 100 mm, and plasma is restricted between the electrodes in a volume of 1.4 cm^3. The output power of the supply was 10 W. Lissajous figures were used to determine the power dissipation in the reactor. This is the plot of charge as a function of the applied voltage through one period. Power absorbed by the plasma is calculated as ~3 W. Unless otherwise stated, a total gas flow rate of 100 mL/min was used for a gas mixture containing 10% hexane and 8% oxygen in helium. The dielectric reactor wall, 1 mm thick, makes the plasma current almost independent of the gas mixture, and spark formation is inhibited. A thermocouple outside the quartz tube reactor was used to control the temperature of the furnace. Light emission from the discharge was collected through a collimating lens in a 90° angle to the outside of reactor at room temperature. An optical fiber transmits the light into an optical emission spectrometer (HR 4000, Ocean Optics) which was connected to a PC for analysis of the spectra.

A scheme of the setup is shown in Figure 2. Mass-flow controllers (Brooks) were used to control the flow rates of gases. Two electrically actuated four-port valves (Valco) were used to switch the reaction mixture to a bypass line to measure the composition of the feed. A Dionex dual gradient P680 HPLC pump was used to dose liquid hexane at an accurate rate. Hexane was evaporated in a cylindrical evaporator operated at a temperature of 130 °C. The temperature of all lines of the setup was kept constant at 130 °C to avoid condensation of hexane.

An elaborate micro-GC system was applied for full analysis of C1 until C8 hydrocarbons, including paraffins and olefins. The online analysis system consisted of two micro-GCs (Varian CP4900). The first micro-GC is a quad system consisting of four channels with four different columns: column 1 is a Molsieve 5A Plot (He carrier gas) for the separation of O_2, N_2, CH_4, and CO; column 2 a PoraPlot Q column for the separation of CO_2, C_2H_6, C_2H_4, H_2O; column 3 an Alumina KCl Plot at T = 80 °C for the separation of C3 and C4 hydrocarbons (paraffins and olefins); column 4 an Alumina KCl Plot at T = 160 °C for the separation of C5 hydrocarbons (paraffins and olefins). The second Micro GC is a dual system consisting of two channels of two different columns: column 1 is a Molsieve 5A Plot (Ar carrier gas) for the separation of He and H_2, and column 2 a CP-SIL 5CB to separate C6−C8 hydrocarbons (paraffins and olefins). All channels contain TCD detectors.

A gas mixture of known concentration of C1−C6 hydrocarbons (paraffins, olefins) was used for the calibration of the micro-GCs. Hexane conversion was calculated on a carbon mol basis i.e., 100% × (6•C6 mols in − 6•C6 mols out)/(6•C6 mols in). There was no carbon deposition during the course of the experiments, and the carbon balance closed between 100 and 110%. The selectivity to individual products is calculated based on the number of moles of carbon contained in a specific product, divided by the total number of moles of carbon in the product mixture (i.e., excluding unconverted hexane).

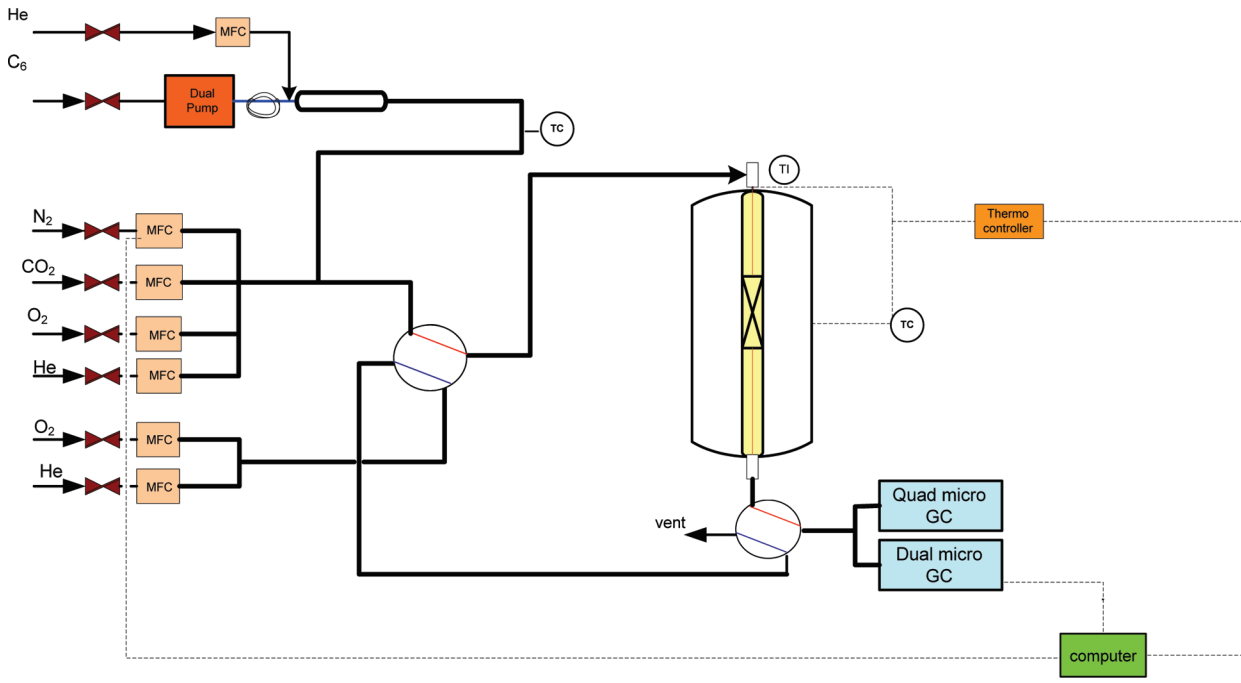

Figure 2. A schematic representation of the measurement setup.

3. Results and Discussion

In a DBD application, most ionized species decay before any major chemical change occur; therefore free radical chemistry involving atoms, molecular fragments, and excited species sets the following chemical processes. In the beginning of discharge formation at atmospheric pressure, electrons reach equilibrium conditions in the electric fields within picoseconds and microdischarges occur at nanoseconds while the free radical reactions may reach equilibrium conditions in milliseconds.[12] Radicals and excited species are generated by electron molecule collisions.[13] Different excitation processes by electron impact are possible: ionization, dissociation, electronic, vibrational, and rotational/translational excitation. Therefore, energy dissipation into various excitation processes sets the initial conditions for the ensuing chemical reactions. In order to understand electron energy distribution in a DBD reactor and energy deposition into various electron molecule collision properties during oxidative conversion of hexane, the Boltzmann equation (BE) was solved by BOLSIG+. The solver can provide steady-state solutions of the BE for electrons in a uniform electric field using the classical two-term expansion.[14] Solving the BE over a range of reduced electric field *E*/*n* (electric field to gas number density ratio represented in units of townsend, Td corresponding to 10^{-17} V cm^2) values determine the average electron energy, energy fractions in collision processes, and reaction-rate coefficients.

BOLSIG+ requires elastic and inelastic electron impact collision cross section data for hexane, oxygen, and helium in order to solve BE for our experimental conditions. Electron impact collision cross section data for oxygen and helium were obtained from the Siglo database.[15] However, to the best of our knowledge, cross sections of collision processes of hexane are not tabulated in the literature. Therefore, we shall confine ourselves to doubled cross sections for propane (proportional to the number of carbon atoms in the molecule) data using additivity rules to estimate electron impact cross section data of hexane.[16−18] It is important to note that analysis of total ionization cross section data for C_xH_y molecules ($x = 1-3$; $1 \leq y \leq 2x + 2$) has indicated that the x linearity of these cross sections can be extended down to low (∼20−30 eV) energies and the additivity rules for chemical bonds have been shown to manifest themselves in linear x and y dependencies of total and partial cross sections of other electron impact processes as well.[19,20] Implementing doubled cross sections of propane for the cross sections of hexane would roughly reflect its peculiarities in the calculation of electron energies and general trends of plasma energy dissipation into different excitation processes. Total ionization cross sections, total dissociative excitation, and vibrational excitation cross sections for the $e + C_3H_8$ system have been determined by the analytic expressions given in ref 20 and the data reported in the literature.[21−23]

Dissociation of hexane in the presence of oxygen with nonequilibrium cold discharge represents complex plasma chemistry. Initial reactions of oxidative conversion of hexane with plasma start with collisions of hexane and oxygen molecules with electrons having energy absorbed from electrical field immediately. However, it is useful to consider changes in certain features of the dissociation pattern of hexane to yield olefin products with varying parameters such as temperature, oxygen ratio, and helium flow rate.

3.1. Effect of Oxygen Addition. Figure 3a shows the effect of plasma and oxygen addition on the conversion of hexane at 600 °C. In the absence of plasma and oxygen, hexane conversion is negligibly small at the present conditions. In the absence of plasma, the presence of oxygen in the feed enhances hexane conversion up to ∼3% and this is the essence of oxidative conversion. Homogeneous activation occurs starting with hydrogen abstraction by oxygen molecules to form $HO_2^{\bullet}$ and hexyl radicals[24]

$$C_6H_{14} + O_2 \rightarrow C_6H_{13}^{\bullet} + HO_2^{\bullet} \quad (1)$$

Plasma alone without oxygen, increases hexane conversion up to ∼7%. Dissociation of hexane is the result of dissociative excitation with electrons. Only collisions with species that have sufficiently high energy would break hexane molecules at C−C (bond energy 3.17 eV) and C−H (bond energy 3.97 eV) single bonds sites. Solving the BE over the reduced electric field (115 Td as calculated for the present reactor configuration) for the hexane + helium plasma system gives average electron energy value of approximately 4.4 eV. This calculation shows the fact that electron energies of impacted electrons in the plasma system are sufficient to crack C−C as well as C−H bonds in hexane molecules. Additionally, the optical emission spectrum of hexane + helium mixture plasma shows the features of electronic excitation of CH radical corresponding to the $A^2\Delta \rightarrow X^2\pi$ transition at 431.15 nm and bands corresponding to H radicals, together with helium lines (see Figure 4). Existence of these bands is the result of dissociative and electronic excitations of hexane and helium, respectively. It is assumed that there are kinetically different modes of hexane activation in relations between total energy of the molecule, threshold energy needed in a certain position, and the probability of dissociation of the activated molecule.[10] In the case of collision processes of propane, the main electron impact dissociative excitation channels are the ones that occur with C−H and C−C bond cleavages to yield propyl, hydrogen, and methane species.[20] In analogy with the case of propane, one may assume that initial reactions involved in the plasma dissociation of hexane are dissociative excitation with energetic electrons, energy transfer from metastable helium species, leading to hydrogen abstraction from hexane to yield hexyl, and hydrogen radicals since these are the direct products of cracking C−H bonds. The hexyl radicals that fragment during initial dissociation process are believed to follow dissociation patterns which form olefins. It was found that the hexyl radicals were thermally unstable above 290 °C, following the decomposition path[25]

$$C_6H_{13}^{\bullet} \rightarrow \text{olefin} + R^{\bullet} \quad (2)$$

When hexane is dissociated by dielectric barrier discharge, initial dissociation products are exposed to a temperature of 600 °C. Therefore, thermal dissociation of hexyl radical would occur in the discharge region. Dimers of hexyl radical are not detected in the product mixture due to the high temperature favoring dissociation rather than recombination of radicals at the present conditions. Moreover, breaking of C1−C2, C2−C3, and C3−C3 σ bonds of hexane will result in the production of radicals which lead to stable hydrocarbon species.[8] Investigation of the dissociation of hexane after bombardment with electrons having 30 eV in a mass spectrometer yielded evidence for C−C bond cleavage.[26] Under collisions with electrons having energies greater than C−C bond, dissociated ions having two, three, and four carbon atoms were found to be more abundant than nondissociated ions and ions containing one or five carbon atoms. Various constituents (CH_3, C_2H_5, C_3H_3, C_3H_5, C_3H_7, C_4H_9, C_5H_9, C_5H_{11}, H, H_2, C_2H_4, C_2H_6, C_3H_6, C_3H_8, C_4H_8) of

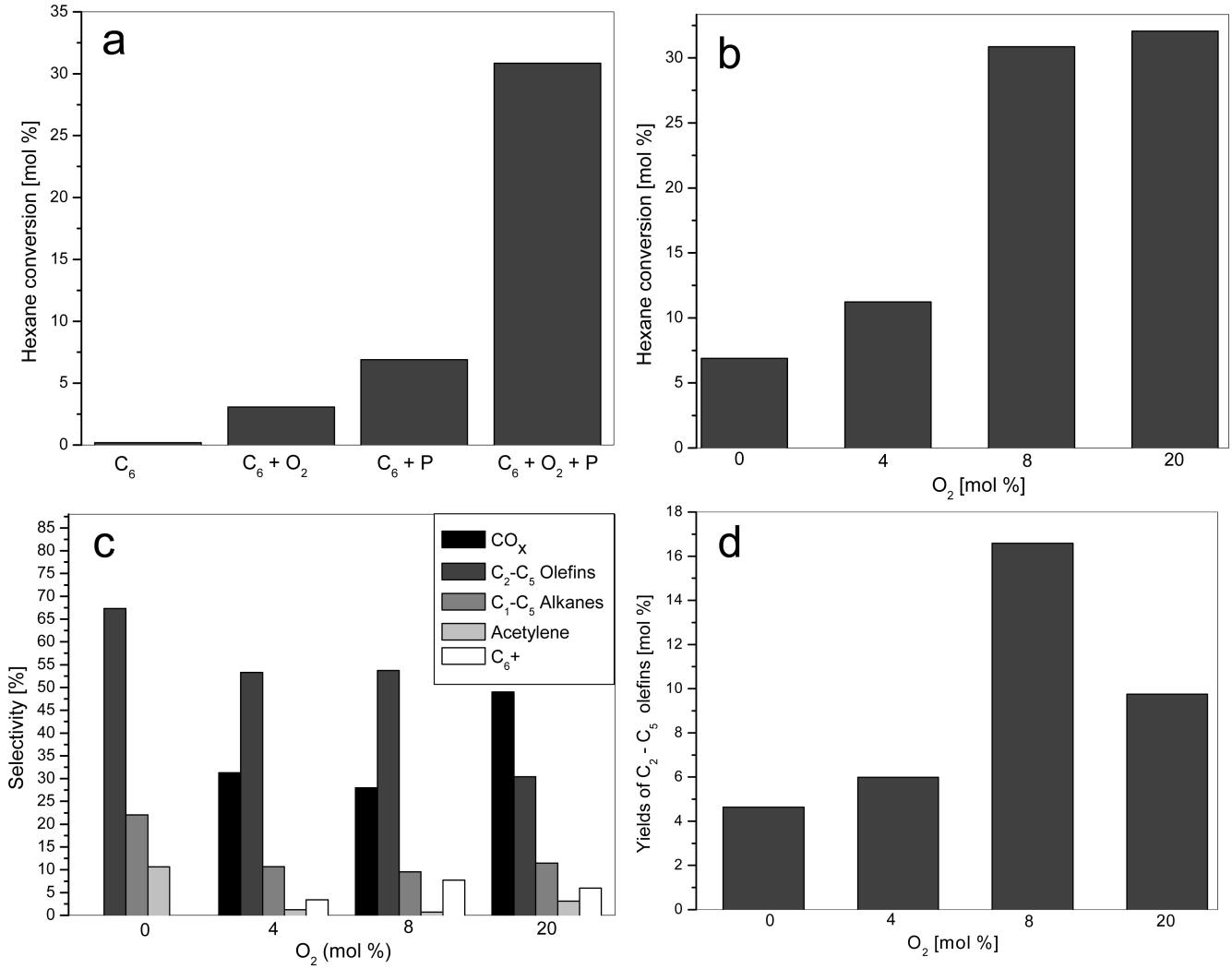

Figure 3. Effect of plasma and oxygen addition on the conversion of hexane at 600 °C (a) (C_6, 10 mL/min hexane + 90 mL/min helium in the absence of plasma; $C_6 + O_2$, 10 mL/min hexane + 8 mL/min oxygen and 82 mL/min helium in the absence of plasma; C_6 + P, 10 mL/min hexane + 90 mL/min helium with plasma activation; $C_6 + O_2$ + P, 10 mL/min hexane + 8 mL/min oxygen and 82 mL/min helium with plasma activation); change in conversion of hexane with increasing concentration of oxygen (b), effect of increasing oxygen concentrations on product selectivities (c), effect of increasing oxygen concentrations on the yields of C_2-C_5 olefins (d). Note that total flow rate is 100 mL/min.

the dissociation products in hexane are supposed to form in the dielectric barrier discharge reactor studied in this work. After initial electron impact dissociation reactions with hexane, radicals and molecules are further involved in hydrogen abstraction, addition, radical decomposition, and recombination reactions determining product distribution.

Introduction of oxygen (8 mol %) in the plasma hexane (10 mol %) system dramatically increases the hexane conversion up to 31% as can be seen in Figure 3a. The results clearly indicate the existence of a new route for hexane conversion involving activation of gas phase oxygen by plasma. The primary event in the plasma oxidative cracking of hexane is the electron impact excitation of molecular oxygen yielding atomic oxygen radicals in the ground $O(^3P)$ and excited $O(^1D)$ states.[9,27] The Franck−Condon region for excitation from the ground state of O_2 is reported to favor a 6 eV and an 8.4 eV process leading to dissociation via electronic transitions to the Herzberg ($A\,^3\Sigma^+_u$, $A^3\Delta_u$,$c^1\Sigma_u^-$) and Schumann−Runge ($B\,^3\Sigma^-_u$) systems[28]

$$O_2 + e \rightarrow O_2(A^3\Sigma_u^+) \rightarrow O(^3P) + O(^3P) + e \qquad (3)$$

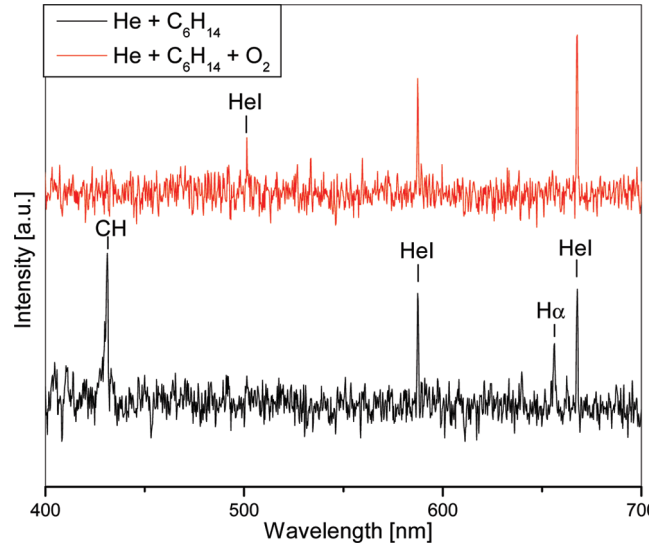

Figure 4. Optical emission spectra of the plasma system, He + C_6H_{14} (10 mL/min hexane + 90 mL/min helium) and He + C_6H_{14} + O_2 (10 mL/min hexane + 8 mL/min oxygen and 82 mL/min helium).

$$O_2 + e \rightarrow O_2(B^3\Sigma_u^-) \rightarrow O(^3P) + O(^1D) + e \quad (4)$$

In a pure oxygen discharge, Boltzmann equation calculations show that reactions 3 and 4 can take place within nanoseconds of current pulse and the excited $O(^1D)$ atoms are converted to the ground state $O(^3P)$ in approximately 10 ns[28]

$$O(^1D) + M \rightarrow O(^3P) + M \quad (5)$$

Here, M refers to the third body collision partner such as hexane, oxygen, or helium. In the presence of hexane, a new pathway is opened for the decay of atomic oxygen radicals, $O(^1D)$ and $O(^3P)$. The oxygen atom $O(^3P)$ was suggested to react with molecules of saturated hydrocarbons to form hydrocarbon and hydroxyl radicals by simply abstracting hydrogen[9,29]

$$C_6H_{14} + O(^3P) \rightarrow C_6H_{13}^{\bullet} + OH^{\bullet} \quad (6)$$

Thus, addition of oxygen to the discharge system promotes the formation of free oxygen radicals, replacing or adding chain initiation and propagation steps by faster steps involving oxygen radicals formed on electron impact on oxygen molecules. As a result, hexane conversion increases significantly. An alternative path for O_2 activation is the reactions between oxygen molecules and hydrocarbon radicals formed upon electron impact dissociation of hexane. In the case of activation of O_2 with hexyl radical, OOH radicals can be formed

$$C_6H_{13} + O_2 \rightarrow C_6H_{12} + OOH^{\bullet} \quad (7)$$

Formation of OOH radicals can further speed up and increase the radical concentration during oxidative conversion. Figure 3b shows the change in conversion of hexane with increasing concentration of oxygen. Further increase in oxygen mole fraction from 8% to 20% results in increase of hexane conversion from 31% to 32%. With increasing the amount of free oxygen radicals, hexane conversion would increase. However, at the same applied power, oxygen dissociation reaches saturation, i.e., 100% oxygen conversion, in the case of 8% O_2 and further increase in the concentration of oxygen has little effect on hexane conversion.

Figure 3c shows the effect of increasing oxygen concentrations on product selectivities. In the absence of oxygen, the main products are C_2-C_5 olefins (olefins with carbon numbers between 2 and 5), C_1-C_5 alkanes (alkanes with carbon number between 1 and 5) and acetylene. C_2-C_5 olefins have a total selectivity value of 67%. The selectivity of olefins with six carbon atoms is very small. Thus, the main reaction pathway is plasma cracking. In the presence of oxygen, CO_x (CO and CO_2) and C_6^+ (hydrocarbons with carbon numbers ≥ 6) appear in the products and olefin selectivity decreases. Increase in oxygen concentration in the feed from 4% to 20% results in increasing selectivity to CO_x and C_6^+. These results show that in the presence of high oxygen concentrations, hexane conversion increases; however, the main reaction pathway is shifted to complete oxidation. Formation of oxygenates is not observed due to cracking conditions at a temperature of 600 °C. Observation of a small amount of C_6^+ is due to dehydrogenation of hexane as well as formation of higher hydrocarbons via coupling of radicals in the postdischarge region which has a relatively lower temperature. Acetylene can be formed by extensive dehydrogenation of ethane and ethylene,[6,7] as well as dimerization of CH type species which was also suggested in plasma methane conversions.[30] It is important to note that acetylene selectivity decreases from 11% in the absence of oxygen to 1% with addition of 4% oxygen. The presence of oxygen can enhance combustion of CH radicals and as a result of this fact disappearance of the CH excitation line is also observed in the emission spectrum as shown in Figure 4. Acetylene formation is less than 1% at 8% oxygen concentration (100% oxygen conversion), and this fact suggests that at limiting oxygen conditions, acetylene formation is minimized.

Figure 3d shows the effect of increasing oxygen concentrations on the yields of C_2-C_5 olefins. The optimum olefin yield that has been achieved was 17% at an oxygen concentration of 8%. A further increase in oxygen concentration to 20% is detrimental to total olefin yields due to a change in the distribution of reaction products toward CO_x.

Figure 5a shows the calculated average electron energy in the helium (82 mol %) + oxygen (8 mol %) + hexane (10 mol %) discharge system as a function of reduced electric field (E/n). In plasma processing, the rate coefficients of electron-impact dissociation reactions strongly depend on the mean electron energy. In the microdischarges, electrons gain a drift velocity and average energy corresponding to an effective E/n, as the value of the electric field E divided by the total gas density n.[31] The effective electric field has been calculated to be 115 Td. For E/n around 115×10^{-17} V cm^2, the corresponding electron mean energy is around 4.3 eV. Dissipation of a fraction of the energy in the electron impact processes leading to vibrational excitation, dissociation, inelastic (nondissociative electronic excitation), and ionization of hexane and oxygen as a function of average kinetic energy of electrons in the same plasma system is shown in Figure 5b and 5c, respectively. In the low electron energy range, typically up to 1 eV, a large fraction of energy is spent in vibrational excitation of hexane and oxygen. The calculated electron mean energy (4.3 eV) is optimal for electron impact dissociation of oxygen and hexane, leading to the formation of oxygen and hydrocarbon radicals, respectively. Figure 4d shows the values for calculated fractional energy dissipation into oxygen dissociation as a function of increasing oxygen fraction in the feed. Increasing the oxygen concentration can have two important consequences for the plasma chemistry. First, the average electron energy can change with varying gas composition and, second, the percentage of energy fraction spent on dissociative excitation processes on oxygen can increase. The average electron energy slightly decreases from 4.4 to 4.1 eV on increasing the oxygen concentration from 0% to 20% whereas the percentage of energy spent on oxygen dissociation increases up to about 14% in the case of 20% oxygen in the feed as can be seen in Figure 4d. The increase of the energy fraction used for oxygen dissociation is the main cause of the increase in hexane and oxygen conversion. Full conversion of oxygen has been reached in the case of 8% oxygen in the feed where the optimum olefin yield has been obtained (Figure 3d). A further increase of oxygen concentration to 20% increases the selectivity to CO_x.

3.2. Effect of Temperature. Figure 6a shows how conversion of hexane and oxygen change when temperature is increased from 400 to 600 °C. The conversion values in the absence of plasma are shown as well. Plasma chemical conversion of hexane is independent of temperature; however, the slight increase at 600 °C is attributed to the fact that at this temperature oxygen conversion reaches 100%. At temperatures above 575 °C, homogeneous activation of hexane by oxygen

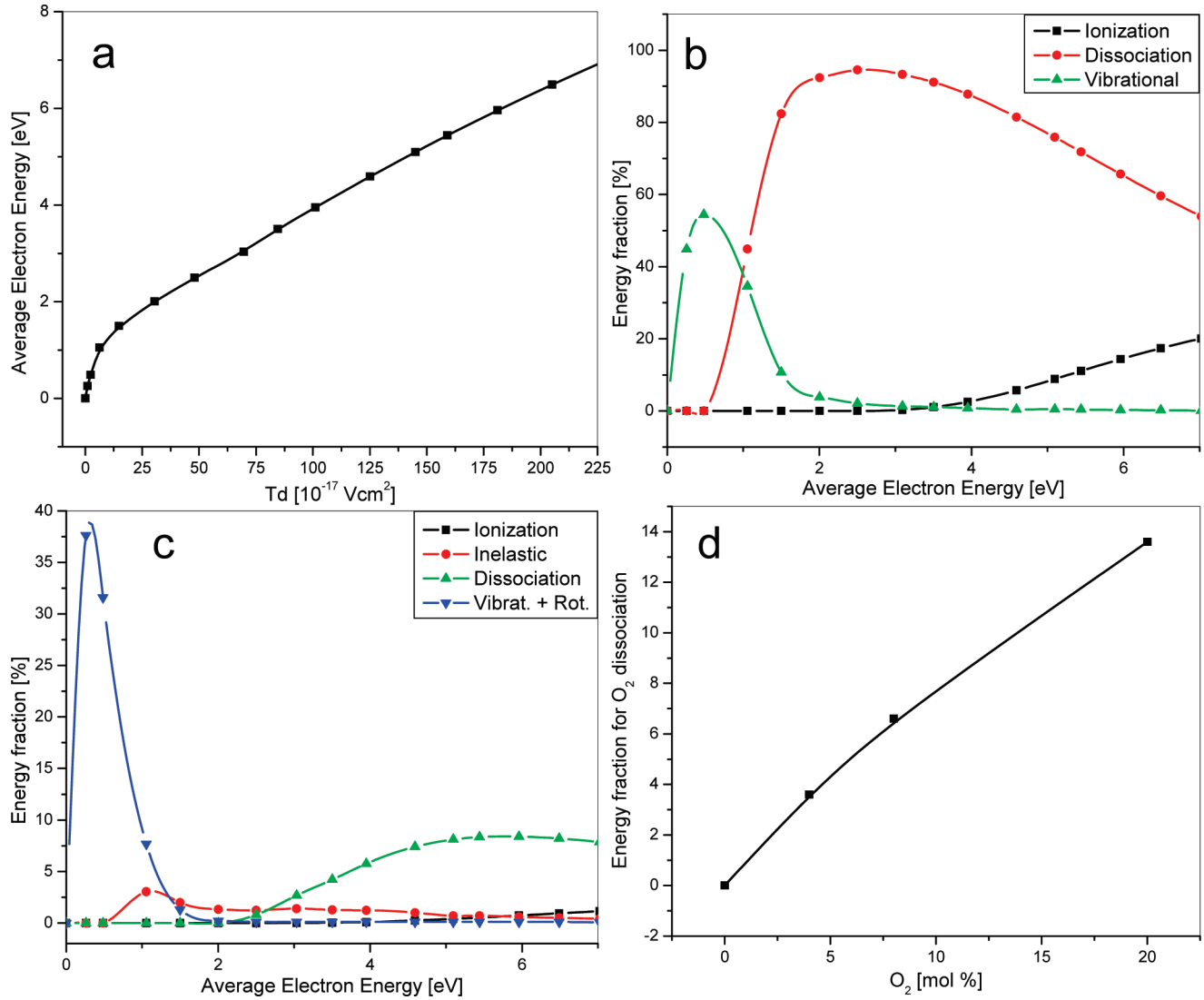

Figure 5. Calculated average electron energy in helium (82 mol %) + oxygen (8 mol %) + hexane (10 mol %) discharge system as a function of reduced electric field (*E*/*n*) (a), dissipation of fraction of energy in the electron impact processes leading to vibrational excitation, dissociation, inelastic (nondissociative electronic excitation), and ionization of hexane (b) and oxygen (c) as a function of average kinetic energy of electrons in the same plasma system and calculated fractional energy dissipation into oxygen dissociation as a function of increasing oxygen fraction in the feed (d).

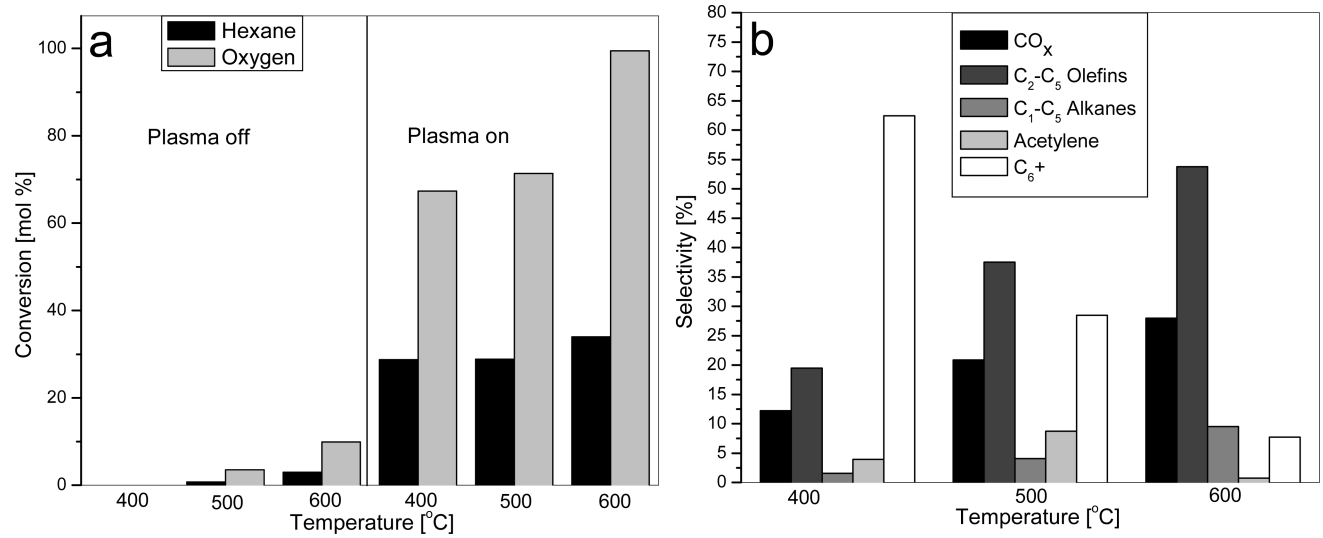

Figure 6. Effect of temperature on the conversion of hexane and oxygen in the plasma reactor (a) and corresponding selectivity values with the plasma on (b).

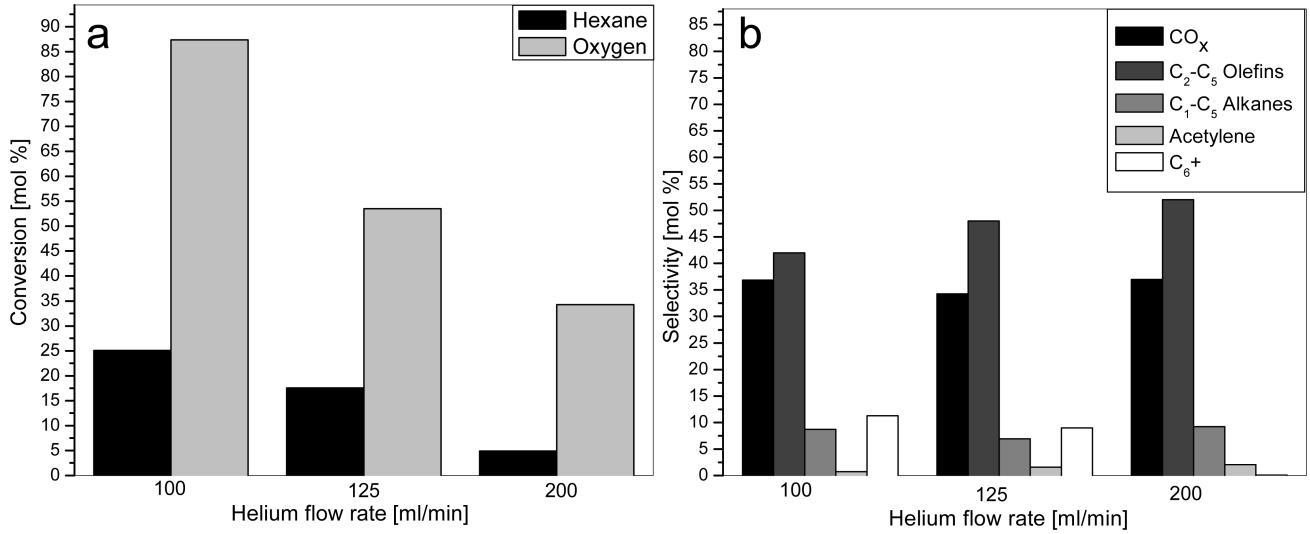

Figure 7. Effect of helium flow rate on conversion of hexane and oxygen (a) and product selectivities (b).

molecules occurs;[24] therefore thermal activation effects are accelerated at 600 °C, increasing hexane and oxygen conversion. Figure 6b shows the corresponding selectivity values for temperatures between 400 and 600 °C with the plasma on. The temperature influences the product distribution significantly. The values at thermodynamic equilibrium are calculated using Chemkin Collection and STANJAN.[32] According to chemical equilibrium state calculations for the gas mixture at temperatures between 400 and 600 °C, hexane and oxygen are fully converted. Main carbon containing products are CO_x, methane, and cyclic products as benzene resulting from dehydrogenation of hexane. However, in the case of plasma oxidative conversion of hexane, conversions and product selectivities differ significantly from the chemical equilibrium state. In plasma, at the lower temperature of 400 °C, considerable formation of C_6+ (62% selectivity) and less formation of C_2-C_5 olefins (19% selectivity) have been observed. A lower temperature favors the coupling of radicals to produce higher hydrocarbons in the homogeneous gas phase. C−C bond formation is exothermic, which is why it is favored at lower temperatures. Similarly, during oxidative conversion of propane in the presence of plasma at room temperature, coupling reactions and formation of hydrocarbons with carbon numbers higher than three were observed.[7] At the higher temperature of 600 °C dissociation reactions, running via C−C and C−H bond cleavage, as well as deep oxidation reactions are favored, which explains the higher selectivity to C_2-C_5 olefins and CO_x. It is important to note that due to presence of both thermal and electron induced reactions in plasma chemical conversion of hexane with oxygen at elevated temperatures, there may be many side reactions of radical intermediates. A plasma chemical kinetic model would shed light on those processes.

3.3. Effect of Helium Concentration. Helium is used as diluent gas in the hexane and oxygen feed. It also plays an important role in the plasma chemistry of oxidative hexane conversion. The measured spectrum (Figure 4) of hexane + helium plasma is dominated by He I excitation lines which show the fact that a large number of metastable helium atoms exist in the discharge. The emission peaks of helium decreased when oxygen was introduced into the hexane + helium system as shown in Figure 4. This fact indicates that the energy transfer from metastable helium atoms helps to activate the reactant mixture.[33] Metastable helium species can be created by electron impact transitions from higher electronic states. It is the lightest noble gas with high ionization potential; therefore increasing the concentration of helium in the reactant mixture results in an increase of the average electron temperature. Figure 7a and 7b show the effect of helium flow rate on the conversion of hexane and oxygen and product selectivities, respectively. Helium flow rate determines the concentration of helium in the product mixture. It is important to note that hexane and oxygen flow rates are kept at 10 and 8 mL/min for all conditions. Calculations show that increasing the helium flow rate from 100 to 200 mL/min increases the average electron energy in the plasma from 4.3 to 5.8 eV, respectively. Higher average electron energy promotes dissociation due to an increase in the rate of electron impact reactions. However, increasing the helium flow rate also decreases the residence time of hexane and oxygen in the active discharge region at the same time, and therefore conversion decreases considerably. A higher selectivity to olefins is observed when the helium flow rate increases as can be seen in Figure 7b, which can be explained by the fact that an increase in the concentration of excited helium species and average electron energy may favor cracking rather than coupling of radical reactions, due to energy transfer to the oxygen and hydrocarbon radicals.

4. Conclusions

In the gas phase oxidative conversion of hexane, the application of plasma induces hexane and oxygen activation via electron-impact dissociative excitation, which enhances hexane conversions at temperatures as low as 400 °C. Main routes for hexane dissociation are C−H, C−C bond scission with electron impact and activation of hexane via oxygen radicals. Solving the Boltzmann equation over the reduced electric field for the hexane + oxygen + helium plasma system indicates that the average electron energy is around 4.3 eV, so electron impact mainly causes dissociation of oxygen and hexane, generating oxygen and hydrocarbon radicals, respectively. The product distribution is mainly controlled by the temperature: at 600 °C C−C and C−H bond cleavage leads to cracking products, while at lower temperature of 400 °C, coupling reactions of intermediate radicals become more significant. The optimum olefin yield which has been achieved was 17% at an oxygen concentration of 8%. The olefin yield decreases with further increasing the oxygen concentration due to shifting of the product distribution toward CO_x. Acetylene formation is minimized in oxygen

limiting conditions. Helium has been used as diluent gas; however, it has also an effect on plasma chemistry by transferring energy from its metastable states to oxygen and hexane and by increasing the average electron energy in the plasma. Thus, helium cannot be regarded as an inert diluent in plasma induced oxidative conversion of hexane.

Acknowledgment. This research was supported by the Technology Foundation STW, applied science division of NWO and the technology programme of the Ministry of Economic Affairs, The Netherlands, Project Numbe 06626. The authors also acknowledge Ing. B. Geerdink and K. Altena-Schildkamp for technical support.

Supporting Information Available: Results of chemical equilibrium calculations. This material is available free of charge via the Internet at http://pubs.acs.org.

References and Notes

(1) Ren, T.; Patel, M.; Blok, K. *Energy* **2006**, *31*, 425–451.
(2) Liu, X.; Li, W.; Xu, H.; Chen, Y. *React. Kinet. Catal. Lett.* **2004**, *81*, 203–209.
(3) Ağıral, A.; Groenland, A. W.; Chinthaginjala, J. K.; Seshan, K.; Lefferts, L.; Gardeniers, J. G. E. *J. Phys. D: Appl. Phys.* **2008**, *41*, 194009.
(4) Trionfetti, C.; Ağıral, A.; Gardeniers, J. G. E.; Lefferts, L.; Seshan, K. *ChemPhysChem* **2008**, *9*, 533–537.
(5) Nozaki, T.; Ağıral, A.; Nakase, M.; Okazaki, K. Japanese Patent No. 2009-147043.
(6) Trionfetti, C.; Ağıral, A.; Gardeniers, J. G. E.; Lefferts, L.; Seshan, K. *J. Phys. Chem. C* **2008**, *112*, 4267–4274.
(7) Ağıral, A.; Trionfetti, C.; Lefferts, L.; Seshan, K.; Gardeniers, J. G. E. *Chem. Eng. Technol.* **2008**, *31*, 1116–1123.
(8) Pierce, R. G.; Padron-Wells, G.; Goeckner, M. J. *Plasma Chem. Plasma Process.* **2009**, *29*, 1–11.
(9) Kudryashov, S. V.; Shchegoleva, G. S.; Sirotkina, E. E.; Ryabov, A. Yu. *High Energy Chem.* **2000**, *34*, 112–115, 2.
(10) Coates, A. D. *Department of the Army Project No. 512-10-001, Ballistic Research Laboratories Report No. 1181*, November, 1962.
(11) Xing, Y.; Liu, Z.; Couttenye, R. A.; Willis, W. S.; Suib, S. L.; Fanson, P. T.; Hirata, H.; Ibe, M. *J. Catal.* **2007**, *250*, 67–74.
(12) Eliasson, B.; Egli, W.; Kogelschatz, U. *Pure Appl. Chem.* **1994**, *66, 6*, 1275–1286.
(13) Slovetsky, D. I. *Pure Appl. Chem.* **1988**, *60, 5*, 753–768.
(14) Hagelaar, G. J. M.; Pitchford, L. C. *Plasma Sources Sci. Technol.* **2005**, *14, 4*, 722–733.
(15) Morgan, W. L.; Boeuf, J. P.; Pitchford, L. C. The Siglo Database, CPAT and Kinema; Available through the web: http://www.siglo-kinema.com/database/xsect/siglo.sec, 1995−1998.
(16) Schram, B. L.; Van der Wiel, M. J.; De Heer, F. J.; Moustafa, H. R. *J. Chem. Phys.* **1966**, *44*, 49.
(17) Kozyrev, A. V.; Sitnikov, A. G. *Russ. Phys. J.* **2005**, *48, 1*, 93–101.
(18) Consoli, A.; Benedikt, J.; Von Keudell, A. *J. Phys. Chem. A.* **2008**, *112, 45*, 11319–11329.
(19) Janev, R. K.; Wang, J. G.; Murakami, I.; Kato, T. Report: NIFS-DAT-68; National Institute for Fusion Science: Toki, Japan, October 2001; ISSN .
(20) Janev, R. K.; Reiter, D. *Phys. Plasmas* **2004**, *11, 2*, 780–829.
(21) Tanaka, H.; Tachibana, Y.; Kitajima, M.; Sueoka, O.; Takaki, H.; Hamada, A.; Kimura, M. *Phys. Rev. A* **1999**, *59, 3*, 2006–2015.
(22) Merza, R.; Linder, F. *J. Phys. B: At. Mol. Opt. Phys.* **2003**, *36*, 2921–2941.
(23) Boesten, L.; Dillon, M. A.; Tanaka, H.; Kimura, M.; Sato, H. *J. Phys. B: At. Mol. Opt. Phys.* **1994**, *27*, 1845–1855.
(24) Boyadjian, C.; Lefferts, L.; Seshan, K. *Appl. Catal., A* **2010**, *372, 2*, 167–174.
(25) Norrish, R. *Proc. R. Soc. London* **1958**, *A243*, 435.
(26) Kambara, T. *J. Phys. Soc. Jpn.* **1947**, *2*, 25–31.
(27) Ağıral, A. Ph.D. Thesis, University of Twente, Enschede, The Netherlands, 2009, ISBN 978-90-365-2916-7.
(28) Eliasson, B.; Kogelschatz, U. *J. Phys. B: At. Mol. Phys.* **1986**, *19*, 1241–1247.
(29) Herron, J. T.; Huie, R. E. *J. Phys. Chem. Ref. Data* **1973**, *2, 3*, 467.
(30) Kado, S.; Urasaki, K.; Sekine, Y.; Fujimoto, K.; Nozaki, T.; Okazaki, K. *Fuel* **2003**, *82, 18*, 2291–2297.
(31) Penetrante, B. M.; Bardsley, J. N.; Hsiao, M. C. *Jpn. J. Appl. Phys.* **1997**, *36*, 5007–5017.
(32) Available through the web: http://navier.engr.colostate.edu/tools/equil.html.
(33) Sawada, Y.; Ogawa, S.; Kogoma, M. *J. Phys. D: Appl. Phys.* **1995**, *28*, 1661–1669.

JP104697U